RADC-TR-80-25
Final Technical Report
February 1980

LEVEL

E AND F LAYER H.F. VOLUME BACKSCATTER REFLECTIVITIES

Boston College

Edward N. Richards
William C. McComish

DTIC
ELECTE
MAY 3 0 1980
C

ADA084835

DDC FILE COPY

ROME AIR DEVELOPMENT CENTER
Air Force Systems Command
Griffiss Air Force Base, New York 13441

80 5 27 290

This report has been reviewed by the RADC Public Affairs Office (PA) and is releasable to the National Technical Information Service (NTIS). At NTIS it will be releasable to the general public, including foreign nations.

RADC-TR-80-25 has been reviewed and is approved for publication.

APPROVED: *William F Ring*

WILLIAM F. RING
Project Engineer

APPROVED: *Allan C Schell*

ALLAN C. SCHELL, Chief
Electromagnetic Sciences Division

FOR THE COMMANDER: *John P Huss*

JOHN P. HUSS
Acting Chief, Plans Office

If your address has changed or if you wish to be removed from the RADC mailing list, or if the addressee is no longer employed by your organization, please notify RADC (EEP), Hanscom AFB MA 01731. This will assist us in maintaining a current mailing list.

Do not return this copy. Retain or destroy.

REPORT DOCUMENTATION PAGE	READ INSTRUCTIONS BEFORE COMPLETING FORM
1. REPORT NUMBER RADC-TR-80-25	2. GOVT ACCESSION NO. AD-A084 835	3. RECIPIENT'S CATALOG NUMBER

4. TITLE (and Subtitle) E AND F LAYER H.F. VOLUME BACKSCATTER REFLECTIVITIES	5. TYPE OF REPORT & PERIOD COVERED Final Technical Report. 15 Dec 77 — 31 Dec 79
	6. PERFORMING ORG. REPORT NUMBER BC-SDAL-79-2
7. AUTHOR(s) Edward N. Richards William C. McComish	8. CONTRACT OR GRANT NUMBER(s) F19628-78-C-0036
9. PERFORMING ORGANIZATION NAME AND ADDRESS Boston College Chestnut Hill MA 02167	10. PROGRAM ELEMENT, PROJECT, TASK AREA & WORK UNIT NUMBERS 61102F 23051224
11. CONTROLLING OFFICE NAME AND ADDRESS Deputy for Electronic Technology (EEP) Hanscom AFB MA 01731	12. REPORT DATE Feb 80
	13. NUMBER OF PAGES 38
14. MONITORING AGENCY NAME & ADDRESS(if different from Controlling Office) Same	15. SECURITY CLASS. (of this report) UNCLASSIFIED
	15a. DECLASSIFICATION DOWNGRADING SCHEDULE N/A

16. DISTRIBUTION STATEMENT (of this Report)

Approved for public release; distribution unlimited

17. DISTRIBUTION STATEMENT (of the abstract entered in Block 20, if different from Report)

Same

18. SUPPLEMENTARY NOTES

RADC Project Engineer: William F. Ring (EEP)

19. KEY WORDS (Continue on reverse side if necessary and identify by block number)

Volume Reflectivity	Frequency	Irregularities (Iono-
E Layer	HF Radar	spheric)
F Layer	Geomagnetic	Doppler frequency
Auroral	Actual auroral conditions	Clutter
High latitude	Quiet auroral conditions	

20. ABSTRACT (Continue on reverse side if necessary and identify by block number)

H.F. radar backscatter data from an OTH radar site in northern Maine have been processed to produce estimates of E and F layer volume backscatter reflectivities. Nighttime returns were selected from the months of September and October and were sorted into evening and midnight time segments for active and quiet days. The reflectivities were analyzed for dependence on geomagnetic coordinates, as well as for dependence on frequency and auroral conditions. The frequency (over)

DD FORM 1473 EDITION OF 1 NOV 65 IS OBSOLETE
1 JAN 73

dependence through the 8-19 MHz range was very strong, while no clear geomagnetic correlation could be established.

TABLE OF CONTENTS

LIST OF ILLUSTRATIONS

PREFACE

Accession For	
NTIS GRA&I	☑
DDC TAB	☐
Unannounced	☐
Justification	

By_____

Distribution/

Availability Codes

Dist	Avail and/or special
A	

EVALUATION

The temporal and spatial occurrence of auroral clutter have been
described for an HF backscatter radar. The clutter signals have been
characterized by their intrinsic reflectivities which permit the evalua-
tion of models of auroral clutter which are developed independently.
This effort contributes to Technical Planning Objective 1C Surveillance
by providing a better understanding of the properties of the polar iono-
sphere and technology for system simulation and diagnosis in the presence
of ionospheric irregularities.

The signal processing techniques developed under this effort provide
the necessary methodology and associated software to serve as the basis for
the RADC/EEP support for the testing phase of the Experimental Radar System
that is currently under development by the CONUS OTH-B 414L SPO.

William F. Ring
WILLIAM F. RING
Project Engineer

1. INTRODUCTION

The objective of this study is to estimate the HF radar volume back-scatter reflectivities from E and F region irregularities in the Polar ionosphere. The primary source of data is the Polar Fox II experiment, in which a high power HF backscatter radar was operated in northern Maine from November 1971 through November 1972. The coverage area included the North magnetic pole, with the auroral oval passing through the coverage region at a mean range of 1500 km. The present study makes use of data from the 2200-0800 UT time interval during the months of September and October of 1972.

Ionospheric clutter is a natural phenomenon that can degrade the performance of radar systems designed for high latitude coverage. The sources of ionospheric radar clutter in the E and F regions of the high latitude ionosphere are magnetic field aligned reflecting structures in the electron density field. These structures exhibit motion which imparts a Doppler shift to scattered radar energy. The backscatter cross section of the region of ionospheric irregularities illuminated by an OTH radar may be very large, making the detection of targets, against the resulting clutter background, difficult or impossible.

The physical mechanisms producing the irregularities in the high latitude E and F layers are thought to be different even though the occurrence of both kinds of irregularities can be correlated with the same solar and geophysical phenomena. Irregularities responsible for E layer auroral clutter, originating at altitudes of about 110 km., are commonly understood to be generated by plasma instabilities driven by the horizontal electrojet currents of the auroral E region [Greenwald, 1973]. One of the first studies attempting to develop a quantitative theory of equatorial E region irregularities based upon the two stream plasma instability is due to Farley [1963], where the energy producing the irregularities is supplied by the equatorial electrojet. Further developments in plasma instability theory were stimulated by the shortcomings of the Farley theory, leading to the gradient-drift, or $\underline{E} \times \underline{B}$ cross field instability [Rogister and D'Angelo, 1970; Farley and Balsley, 1973], and an adaptation of these equatorial zone theories to auroral latitudes [Ginzburg, 1970; Ginzburg and Rubadze, 1972].

1

The radar aurora is related to the visual aurora, but significant differences are observed between the two phenomena. Both a discrete and a diffuse type of auroral clutter are observed. The discrete type occurs mostly at nighttime and is characterized by large velocities, while the diffuse type is normally observed during daytime (afternoon) and exhibits slower velocities. It seems that the diffuse radar aurora is related to stable visual auroral arcs; and the discrete radar aurora is related to pulsating rays and moving patches in the visual aurora [Bullough and Kaiser, 1955].

Several models of E region irregularities arising from plasma instabilities have been invoked to explain the range of E region clutter phenomena, particularly its frequency dependence. There has not been as much progress in explaining high latitude F layer clutter. One useful method of studying high latitude F layer irregularities has been by observing scintillations in electromagnetic radiation originating from radio stars and satellites. These scintillations are produced by electron density fluctuations associated with F layer irregularities, and permit observations to be made on the geophysical distribution of these irregularities [Aarons, 1973; Nielson, and Aarons, 1974; Martin and Aarons, 1977].

Another method of observation is the use of H.F. radar backscatter which constitutes the subject of this report. Due to the strong magnetic field alignment of ionospheric plasma irregularities, their radio scatter cross section is highly anisotropic, with a maximum value in the plane orthogonal to the local geomagnetic field direction. In the case of a backscatter radar this means that appreciable radar returns are received only when the propagation direction is closely perpendicular to the geomagnetic field direction. Most of the radar studies of high latitude irregularities have used VHF and UHF transmissions which are insensitive to F layer field aligned irregularities because there is not sufficient refraction to direct the rays perpendicular to the magnetic field at those altitudes. At HF the ionospheric refraction is sufficiently great to permit

2

orthogonality over a large area of radar illumination. This advantage, however, is achieved at the expense of frequent uncertainty about the path of the radar signal, with consequent difficulty in accurately determining the location and size of the scattering region. This difficulty leads, in this report, to a simplification in computing the scattering volume, with a resulting uncertainty in the value of the reflectivity.

2. DESCRIPTION OF EXPERIMENT

The Polar Fox II experiment included the operation of an HF backscatter radar by the Raytheon Company in northern Maine from November 1971 through November 1972. The coverage area is shown in Figure 1. The experiment used a high power radar (800 kW peak) to provide coverage over a 90° azimuthal sector from -30° to +60° azimuth measured from true North. The coverage area included the north magnetic pole, the auroral oval and an area at the most easterly azimuths which could reasonably be expected to be equatorward of the auroral zone. The auroral oval passes through the coverage region at a mean range of 1500 km.

The radar operated at 30 pulses per second with a 10 kHz chirp bandwidth corresponding to 15 km range resolution. Radar parameters are listed in Table 1.

TABLE 1

Radar Parameters

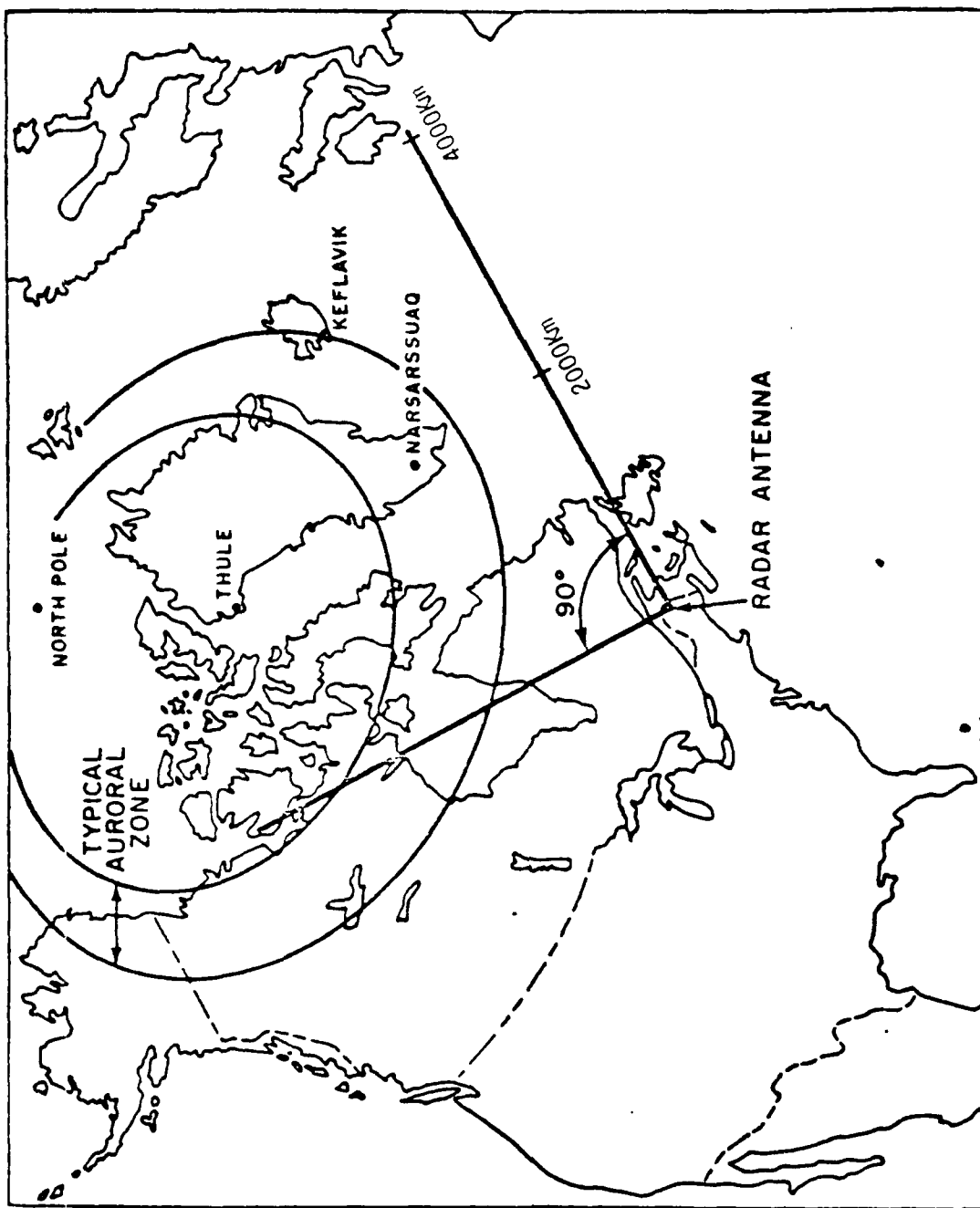|		
Location:	Caribou, Maine	47°N 68°W
Frequency:	6 to 26 MHz	
Power:	64 Kw Avg.	
Range Resolution:	15 km	
Receive Beamwidth:	9 degrees at 10 MHz	
Azimuth:	11 steps from -30°T to +60T	
Measurement:	One minute/Freq./Beam Position/Hour	

Figure 1. Polar Fox II Radar Coverage Map

4

The Polar Fox II radar used a 4 element vertically-polarized log-periodic transmitting antenna array and a 28 element vertically polarized log-periodic receiving area with a nominal 30 dB taper. Antenna pattern measurements were performed in a cooperative program by Raytheon, Lincoln Laboratory [Nichols, 1973] and the Rome Air Development Center [Parry, 1973] using a variety of aircraft. Results of all the measurements were analyzed at Lincoln Laboratory to prepare net gain tables for each antenna referenced to the receiver input or transmitter output including all line and network losses. Gain vs. elevation angle tables were prepared for each antenna for each operating frequency, for each steer angle and for each transmitting system element configuration used. Measured transmit and receive patterns for 3 different frequencies on the antenna boresight (15° true North) are shown in Figure 2.

Radar operations were scheduled for two twenty-four hour runs each week. Three backscatter ionograms, one on boresight and one to east and west of boresight were made each hour. The ionograms covered 6 to 26 MHz in freq., and 1000 to 4000 km in range which is the full operating range of the radar. The three ionograms required about four minutes to complete. These were followed by a series of fixed frequency backscatter surroundings to examine the signal strength and Doppler spectrum as a function of range and azimuth. Three fixed frequencies were selected well in advance using ESSA prediction techniques, to provide backscatter coverage of the 1000-4000 km range in 1000 km increments. The selected frequencies could be changed based on operating experience and using the backscatter ionograms for guidance.

Operations began on the lowest frequency. Data were collected at a given azimuth for one minute, including a one second noise measurement with the transmitter off, and average Doppler spectra computed at each range interval. At the end of each minute the average Doppler spectrum at each range interval was written on magnetic tape. The spectra consisted of 32 values at 15/16 Hz intervals. This measurement was repeated in 10° azimuth increments through the 90° scan sector. This eleven minute sequence was then repeated using the middle frequency selected to provide ground coverage in the 2000-3000 km range, and finally the sequence was repeated at the highest radar frequency for coverage in the 3000-4000 km range. The back-scatter measurement took thirty-three minutes and was repeated once each
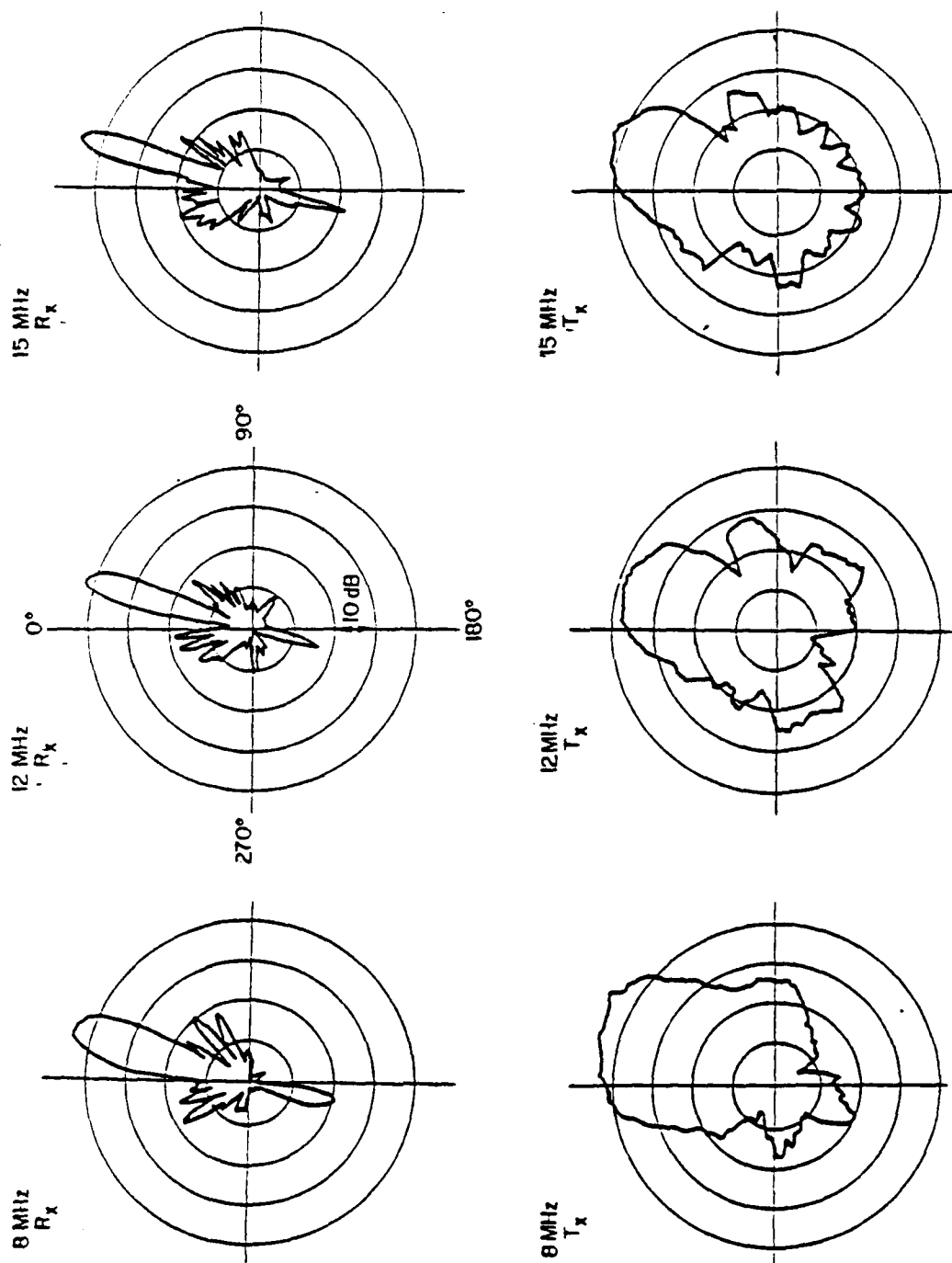
5

Figure 2. Polar Fox II Transmit (Tx) and Receive (Rx) Antenna Patterns for 3 Frequencies

6

hour resulting in a one minute measurement at a particular frequency and azimuth each hour.

3. DATA REDUCTION

3.1 Footprints

The range/Doppler information recorded in each azimuth measurement during the fixed frequency mode of operation was displayed as a footprint as in Figure 3. This is a format in which the Doppler spectrum of the received signal is displayed in each of the 15 km range bins. The footprint is a method for viewing a three-dimensional array in a two-dimensional format, with the amplitude of the received power in -dBW in the appropriate range/ Doppler location as the third coordinate. In another footprint display the numerical values of the amplitude are replaced by letter symbols representing 10 dB increments to aid in the visual discrimination of amplitude levels. These displays are used for the routine mode analysis described below. A three-dimensional plot display, shown in Figure 4, requires a substantial amount of computer time to produce, and is valuable on a limited basis when amplitude variations are small or when clutter patterns are complicated. They are also valuable in making similar clutter patterns among a number of footprints stand out clearly.

Only the data from the fixed frequency mode of operation were available for processing. Recordings of the swept frequency ionograms, produced once each hour just before the fixed frequency scans, were available in poor quality Fax records and were of limited use.

3.2 Threshold and Interference

A threshold level was established for each footprint based upon the noise spectrum of the data. A histogram of the signal levels in a footprint for all range/Doppler cells showed that the number of these noise signals typically decreased with amplitude for about 6 dB above the minimum signal level. This was taken as the population of the noise unrelated to ionospheric or ground clutter, so that the threshold was set 6 dB above the minimum signal level.

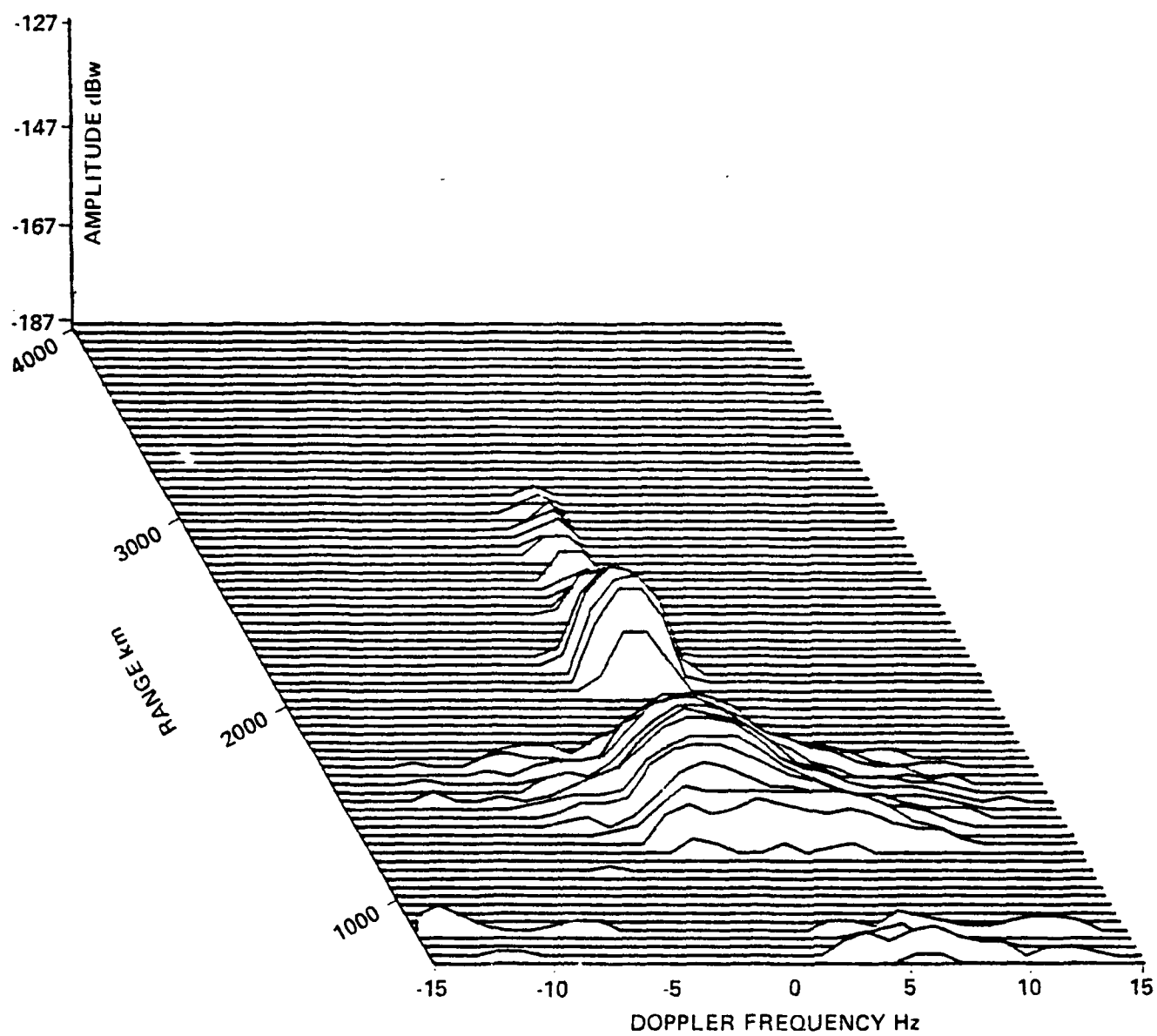Figure 3. Polar Fox II Range/Doppler Footprint

8
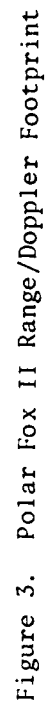
Figure 4. 3-D Plot of Range/Doppler Footprint

Interference from other users of the HF band is frequently present and particularly so in the nighttime hours when the useable band of frequencies is contracting and operators are competing for clear channels. Since the radar was restricted to specific operating frequencies there was a significant amount of interference contamination in the data. This interference usually produced energy in a narrow Doppler band (typically 2 Hz) with constant received power at all ranges, and was often of significant amplitude relative to the clutter.

An algorithm was designed to routinely eliminate these interference lines from the footprints, without raising the noise threshold, with a minimum effect on the overlapping clutter. It made use of the constant amplitude with range, and established when the population of the minimum signal in a Doppler cell, taken over all range bins, exceeded a certain critical level, and was also a critical number of dB above the noise threshold. These critical parameters were determined empirically. An example of the application of the interference algorithm is shown in Figure 5. There were initially three interference lines and it will be noticed that while there is some degradation of the broad clutter, the line at -1 to 0 Hz has been quite clearly eliminated.

Another algorithm was designed to recognize ground clutter in the footprints, a process that was greatly facilitated by the previous removal of interference lines in the region of 0 Hz Doppler. The algorithm makes a parabolic fit to five adjacent amplitudes centered around the peak amplitude in each range bin. The curvature of the parabola is evaluated and examined along with the Doppler frequency of the peak. If the curvature is above an empirically determined critical value, appropriate to the narrow ground spectrum, and if the peak is within ±1 Hz, the signal in the range bin is designated as ground clutter. When the ground clutter occurs along with spread clutter in a range bin, it is eliminated by substituting the average of the clutter values at ±3 Hz before the spread clutter is processed further. This is illustrated in Figure 6.

3.3 Mode Identification

With a range coverage of 625 to 4000 km, the clutter returns in the backscatter data show the effects of a variety of ionospheric conditions.
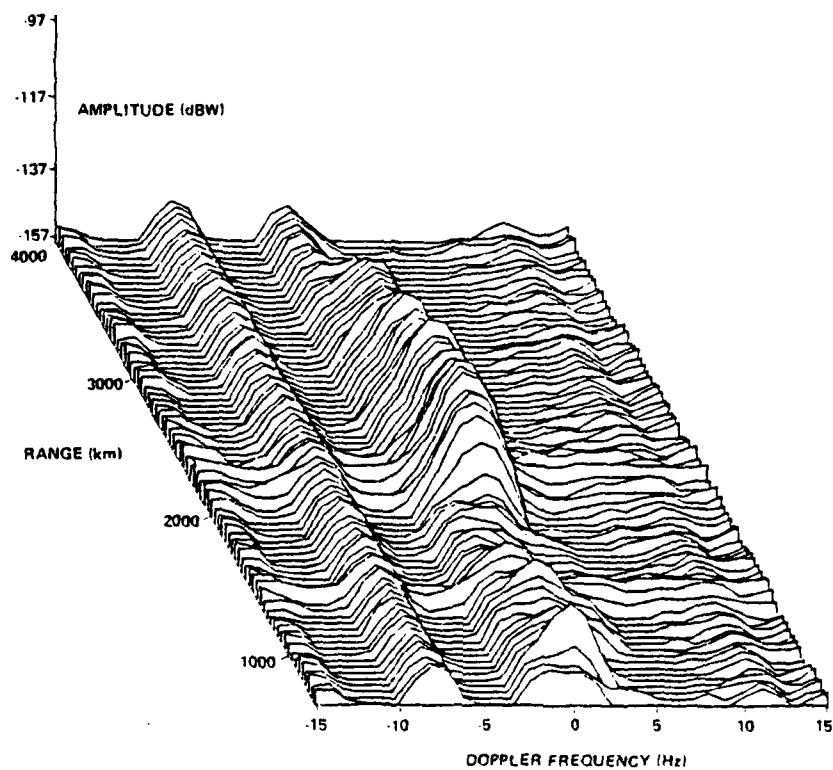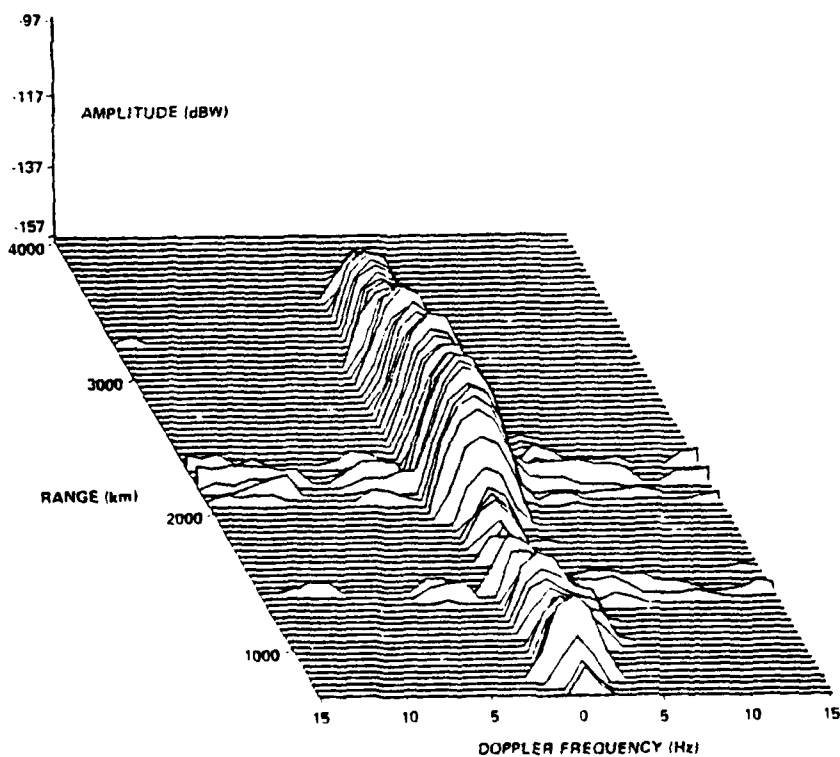
Figure 5a.   Interference Lines Present In Clutter

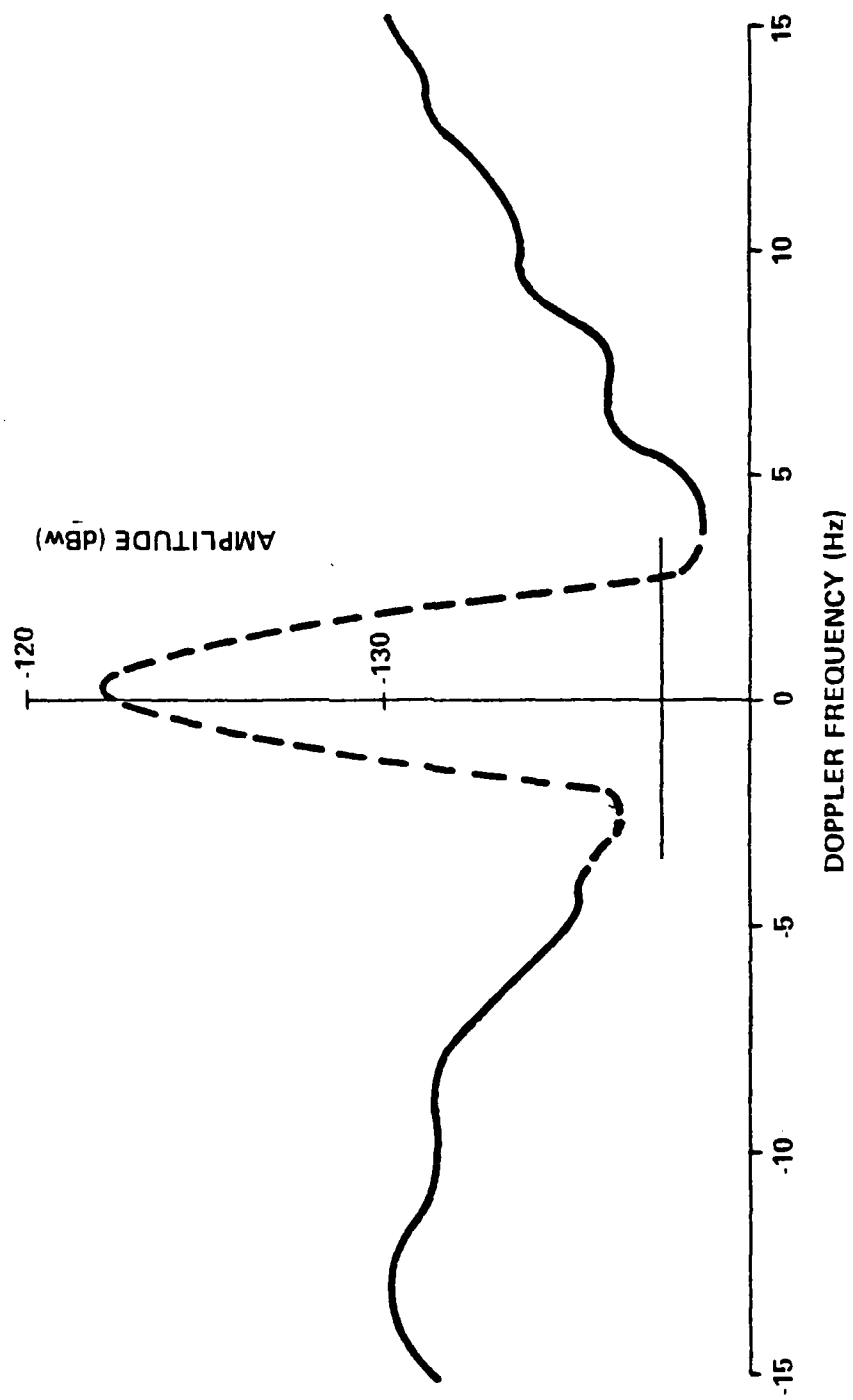Figure 5b.   Interference Lines Removed

AMPLITUDE (dBw)

-120

-130

DOPPLER FREQUENCY (Hz)

-15   -10   -5   0   5   10   15

Figure 6.   Illustration of Ground Clutter Removal

12

They include cases of direct E and F returns, E and F region backscatter after one or two ground reflections, as well as ground backscatter. In order to minimize the ambiguity in the identification of ground/ionosphere propagation modes, it was decided to limit consideration to returns from less than 1500 km range. This would assure a high probability of selecting only direct returns from E or F region clutter sources.

The footprint listings, shown in Figure 3, were the basic data presentation used for mode identification. These footprint displays had a threshold of minimum signal level established, and any interference lines were removed. Mode identification was based essentially upon a visual recognition of more or less distinct clutter regions in the range interval from 625 km to 1500 km. A distinct region of clutter confined to less than 1100 km, the line of sight horizon range for an altitude of 110 km, was designated as E clutter. A distinct region of clutter commencing beyond this range would be designated as F clutter. In the example shown in Figure 3, the close in returns (less than 820) are very likely from the E region. The broad spectrum returns commencing at 1225 km and continuing to nearly 2000 km are designated as F returns. The narrow spectrum returns centered at 0 Hz from the longer ranges are ground clutter. Usually a region of clutter commencing at less than 1100 km and extending well into the F region range without apparent discontinuity would all be designated as F clutter. These fairly simple rules provided the basis for scanning a large quantity of data to produce statistically accurate samples of E and F clutter returns from which to obtain estimates of reflectivities.

Median values of the reflectivities from designated E and F sources did indeed seem to indicate that these two sets of reflectivities constituted two distinct populations. A test was devised to check whether these populations represented two different clutter sources, or whether the distinct populations could have resulted from the different assumptions regarding layer height with consequent antenna gain and ionospheric loss values, made in the computations. Using a five day sample of data, reflectivities of returns which had been designated as E layer clutter were computed using F layer assumptions - i.e., F layer height, and corresponding antenna gain and ionospheric absorption loss. The resulting

13

population was clearly different in median value from that based on the assumption that the reflectivities represented and E layer source. This test increased confidence that the above mode identification criteria led to a statistically valid discrimination of propagation modes, and therefore clutter sources.

4. RADAR EQUATION

The volume backscatter reflectivity is intended to be independent of the specifications of the measuring system and to characterize the intrinsic nature of the auroral backscatter. For the volume reflectivity, it is necessary to define a volume in the ionosphere which contributes to the received power at a specific time delay. The azimuthal beam width and the pulse width define two of the dimensions. The vertical dimension is defined as the angle between two rays orthogonal to magnetic field lines and separated by a range difference equal to the pulse length. This is depicted in Figure 7 and was determined by three dimensional ray tracing using model ionospheres to have a nominal value of 0.5°.

The volume reflectivity is derived from the radar equation as

$$\sigma_0 = \frac{(4\pi)^3 R^4 L_1^2 P_R}{P_T G_T G_R \lambda^2 \text{(Volume)}}$$

where σ_0 = volume reflectivity in m^2/m^3

R = range to clutter

L_1 = propagation loss term (one way) for ionospheric absorption

L_2 = loss term for auroral absorption (one way)

P_R = received power

P_T = transmitted power

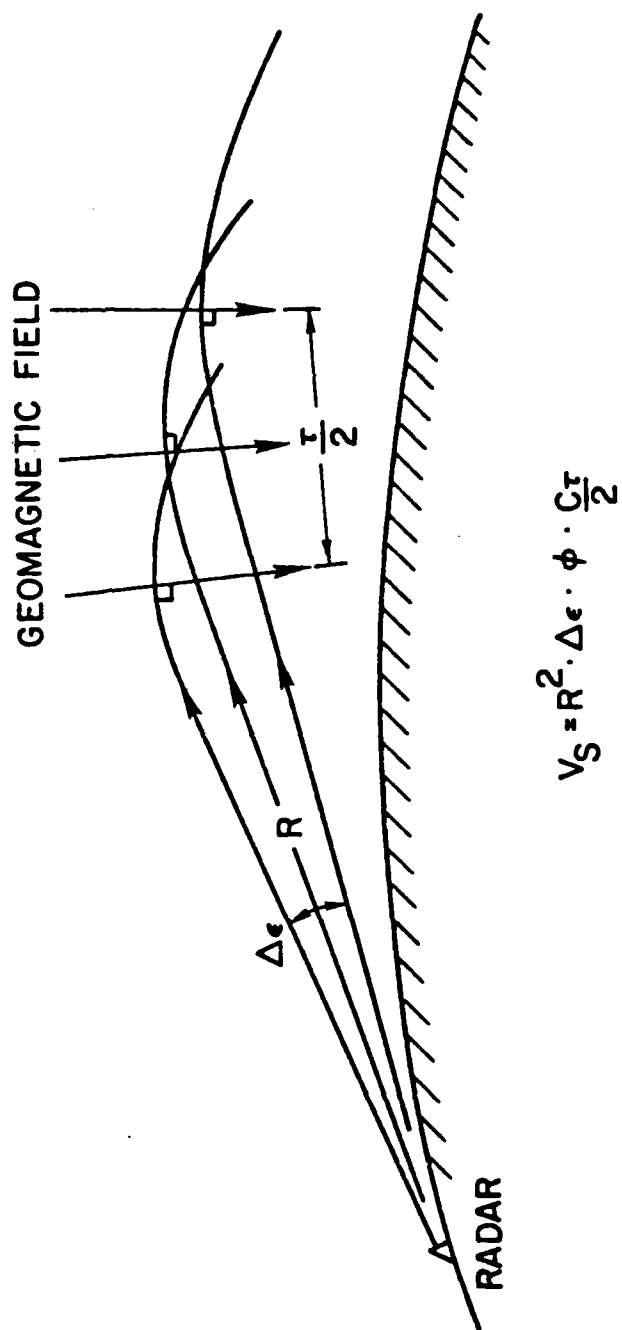G_T = transmitter antenna gain

G_R = receive antenna gain

λ = wavelength

14

$$V_S = R^2 \cdot \Delta\epsilon \cdot \phi \cdot \frac{c\tau}{2}$$

Figure 7. Scatter Volume and Effective Vertical Angle

Illuminated volume $= \frac{c\tau}{2}$ $(R\phi)$ $(R\Delta\epsilon)$ m^3

τ = pulse width

ϕ = azimuthal beamwidth

$\Delta\epsilon$ = effective vertical angle

The loss term L_1 was adapted from a method developed for ionospheric absorption calculations [George and Bradley, 1974].

The auroral absorption loss term L_2 was determined from the model developed by Foppiano [Foppiano, 1975; Vondrak et al, 1978] of monthly median absorption. This is a model of the spatial and temporal variation of the vertical aurora absorption mapped in terms of a coordinate system of corrected geomagnetic latitude, longitude and local time. The locations of D region penetration for E and F height reflections were determined in the geomagnetic coordinate system and used to estimate the vertical absorption at 30 MHz. The zenith angles of the rays were calculated to modify the vertical absorption values by a secant factor and the values were normalized to the frequency of interest through the inverse frequency-squared dependence of non deviative absorption.

5. RESULTS OF ANALYSIS

The returns analyzed here were collected during the months of September and October, 1972, between the hours of 2200 and 0800 UT. Of the nine days of operation during the month of September, data from one day could not be used because the transmitter power was not recorded. The system was also in operation nine days during the month of October, and only the data from several isolated time segments could not be processed due to difficulties in reading the data tapes.

The data from both months were analyzed to study the volume backscatter reflectivity as a function of layer height and frequency. The October data were analyzed in more detail in an attempt to observe any geomagnetic or auroral effects on the reflectivity. In particular, an attempt was made to observe any correlation of reflectivity with geomagnetic coordinates or with auroral conditions relating to the auroral oval.

Using DSMP satellite photographs, four of the nine days of operation in October were designated "active", while the remaining five days were designated "quiet". On the active days, photographs of the auroral zone showed auroral boundaries consistent with a Q between 3 and 4. On the quiet days the auroral boundary in the photographs was consistent with a Q between 0 and 1. Each of these data sets was further separated into evening (2200-0200 UT) and midnight (0300-0800 UT) data. Thus, there were four separately processed sets of data.

Figure 8a. shows the region covered by the Polar Fox II radar, with the southern auroral oval boundaries for active and quiet conditions in the local evening time segment superimposed. Under quiet conditions the boundary misses the closest range segment and divides the farthest two segments into eastern and western azimuthal sectors. The active auroral boundary covers a good portion of the closest range segment at the western azimuths. Figure 8b. shows that under active conditions all range segments are covered by the oval in the midnight time segment.

Each of these sets of data was analyzed for range and azimuth variation which, with the separate time segments, constituted the basis for an attempted correlation with geomagnetic coordinates. At each azimuth a median reflectivity, with upper and lower quartiles, was computed for each of the three range groups of F layer returns, and for the one range group of E layer returns. The range analysis was intended to show any strong correlation with geomagnetic latitude, while the analysis of evening and midnight time segments was intended to show any strong correlations with geomagnetic longitude. No attempt was made to resolve the azimuthal variation into these geomagnetic coordinates.

5.1 Geomagnetic Dependence of Reflectivity

A comparison of simultaneous UHF observations of auroral clutter and high latitude scintillations at F region altitudes [Unger, 1974] indicate that E region and F region clutter sources may have different geomagnetic latitude distributions. It is found that auroral clutter peaks considerable south, geomagnetically, of the most intense scintillations. On the other hand, a comparison of scintillation observations at the same F region
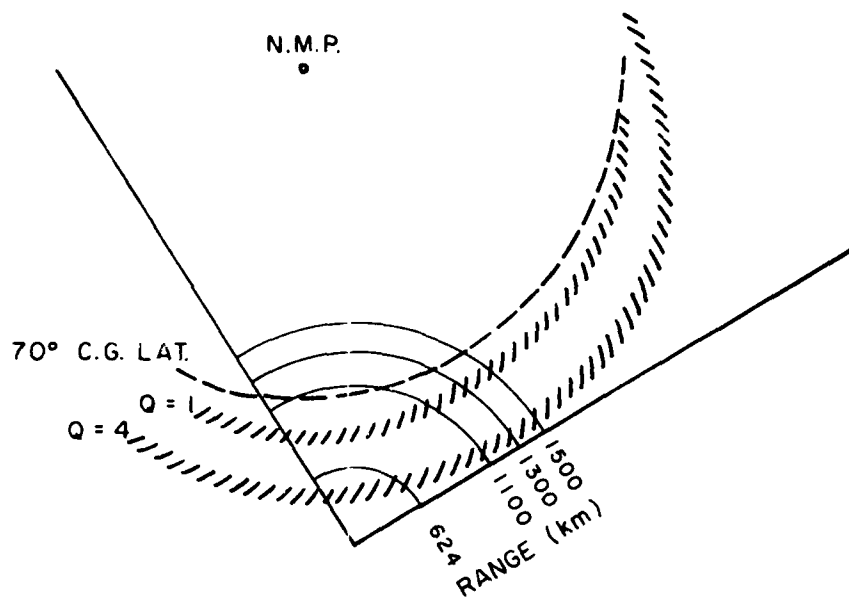
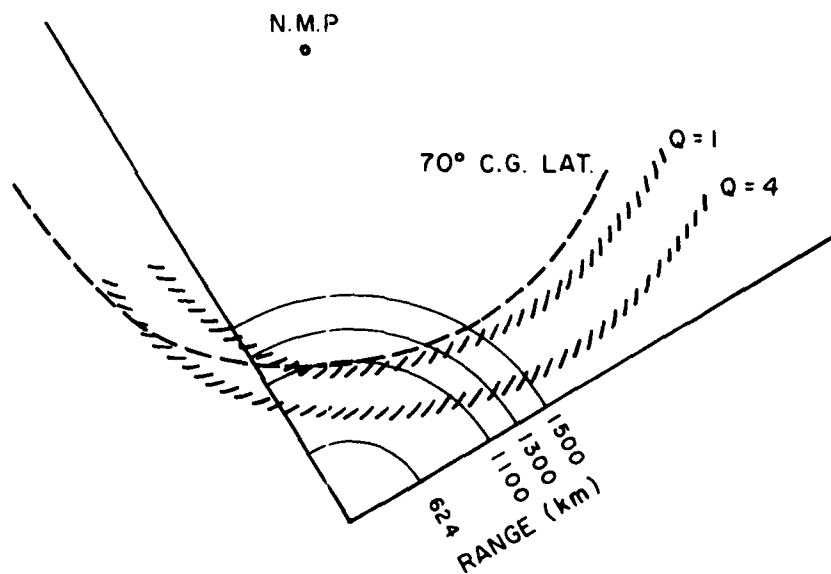Figure 8a. Southern Auroral Boundaries - Local Evening

Figure 8b. Southern Auroral Boundaries - Local Midnight

18

altitudes with the optical aurora observed in DMSP satellite photographs [Martin, 1977] shows a strong geomagnetic correlation. The HF backscatter data reported on here provide simultaneous observations of the same type of both E region and F region ionospheric clutter, perhaps making it possible to better infer a relationship between the two clutter sources.

5.1.1 E Reflectivity

Since the E layer returns originated in only the first range interval, no range variation in the E reflectivity is presented. Figure 9 shows the E reflectivities, under combinations of evening and midnight, and active and quiet conditions, plotted against azimuth at three frequencies. There is some increase in reflectivity at all three frequencies, and a pronounced increase at 8 MHz, toward the western azimuths under quiet midnight conditions. This may be consistent with the fact that the oval partially covers the western sector of the closest range segment. There may be a similar tendency during active evening periods. There was no data available at 8 MHz for active evenings, nor for the eastern azimuths at 12 MHz. Under quiet evening and active midnight conditions the oval either completely misses or completely covers the closest range segment. Nevertheless there are still tendencies for the reflectivity to increase toward the western azimuths. From these data, then, any evidence that the intensity of the irregularities increases in the auroral oval is ambiguous.

It may be observed in Figure 9, showing the number of E layer returns plotted against azimuth for each frequency, that under active midnight conditions the number of events increases toward the west at all frequencies, while no clear trend exists under any of the other sets of conditions. Also Figure 10 shows some consistent tendency for the E layer reflectivities, averaged over azimuth, to be highest under active midnight conditions.

5.1.2 F Reflectivity

In the F layer reflectivity data shown in Figures 10a. and 10b., no consistent azimuthal trend is apparent in any range group under any set of conditions. However, there is an increase in reflectivity with range,
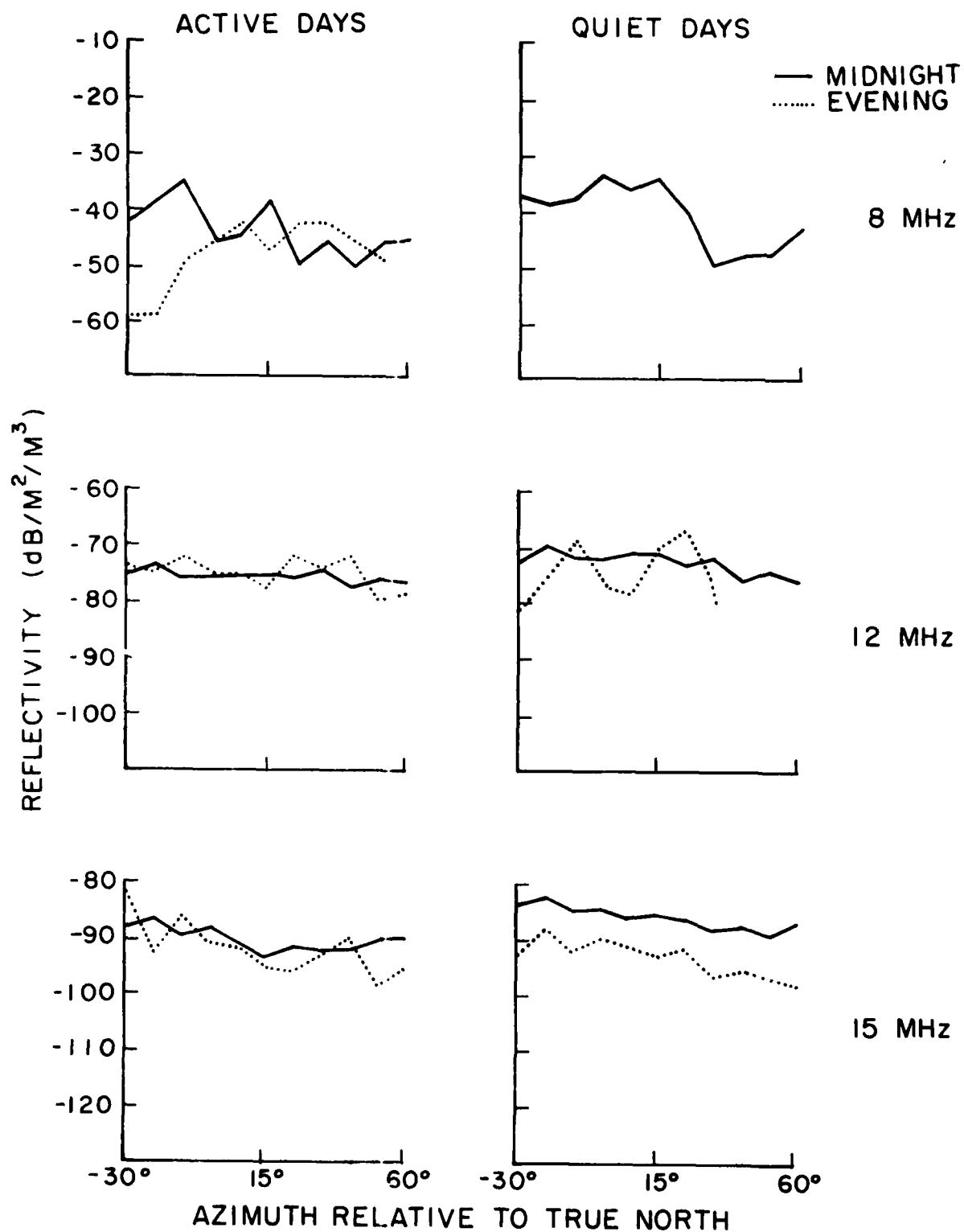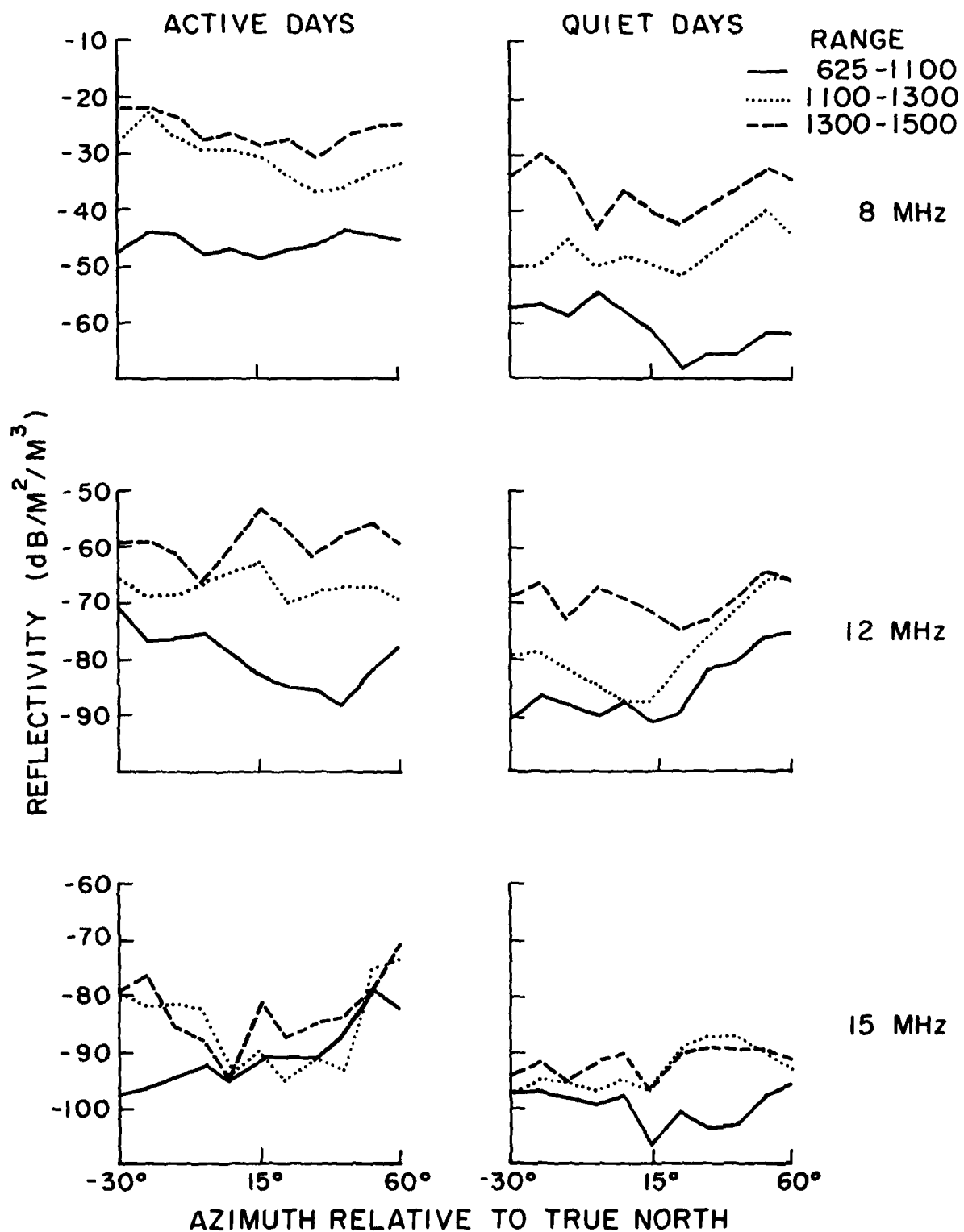
Figure 9. Azimuth Plots of E Region Reflectivities

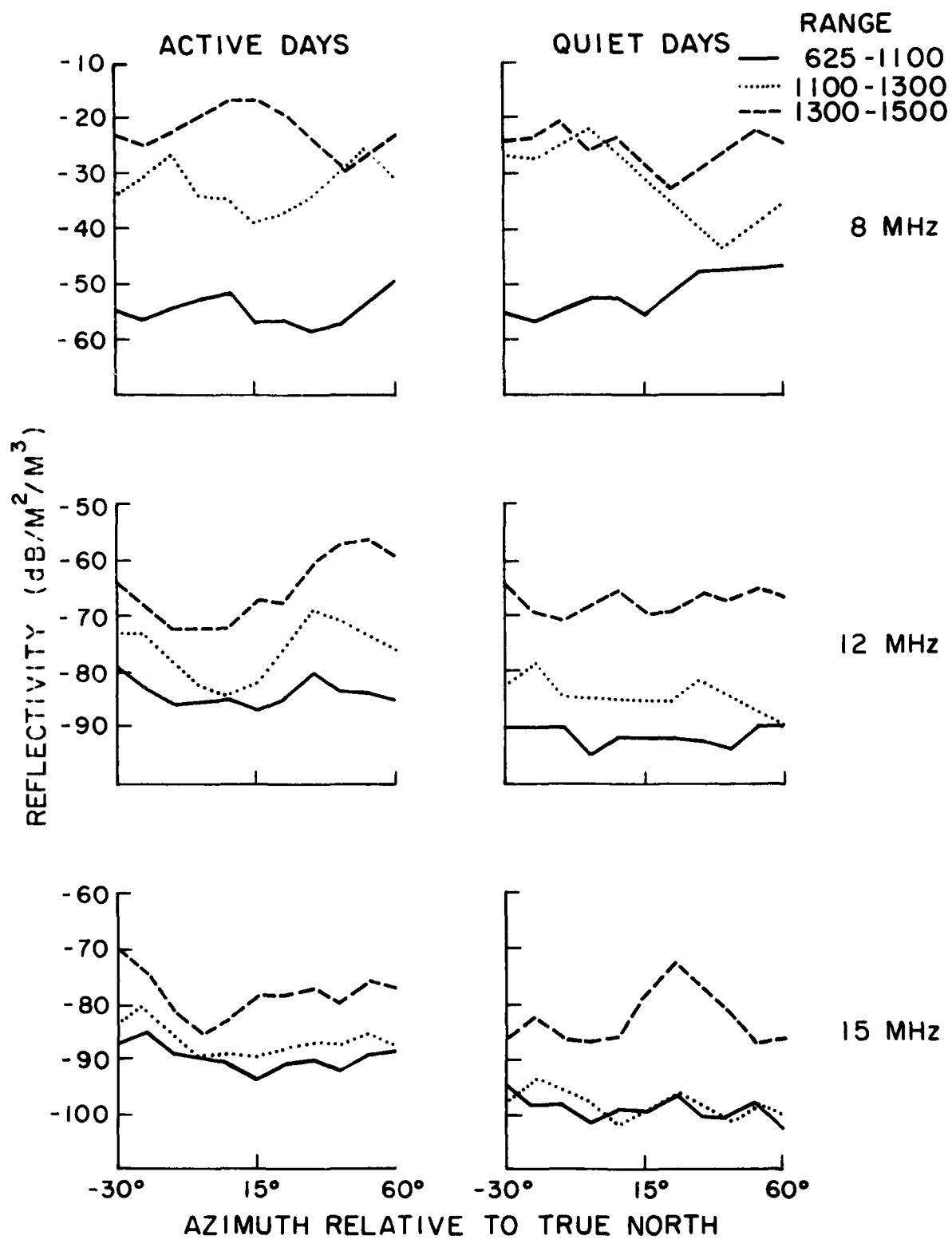Figure 10A. Azimuth Plots of F Region Reflectivities (Evening)

Figure 10B. Azimuth Plots of E Region Reflectivities (Midnight)

under almost all conditions, with the largest increase occurring from the closest to the middle range at 8 and 12 MHz. This seems to be consistent with the supposition that any range increase would be toward regions of more intense irregularities. But an examination of the auroral ovals show that some azimuthal trend in the range increase of reflectivity would be expected, especially where the oval covers only a western portion of the range sectors, if there were a correlation between the auroral oval and the intensity of the irregularities.

In the absence of consistent azimuthal trends in reflectivity, conclusions about the range dependence of the reflectivity are based upon azimuthal averages. It is clear from Figure 11, which shows azimuthal averages of the reflectivity vs. range for both the September and October data, that there is a consistent increase in reflectivity with range at all frequencies, as well as a consistency in the range behavior at each frequency. But without any ordered azimuthal behavior it is difficult to make any correlation with geomagnetic coordinates, or to make a geophysical interpretation.

Other explanations than geophysical ones may be considered for the range variation in the F region reflectivity. It was mentioned above that there was considerable uncertainty in the ray geometry, leading to the assumption of line-of-sight propagation for computing reflectivities. In particular, any error in the scattering volume from this assumption would show up as an incorrect range dependence of the reflectivity. But studies of the effective volume using ray tracing in model ionospheres indicate that the scattering volume at the shortest ranges, particularly just beyond penetration, are underestimated by straight line propagation. The radar equation shows that this would lead to larger rather than smaller values for the reflectivity.

Consideration was also given to the possibility that a poor estimation of reflection heights, giving rise to erroneous elevation angles and therefore to erroneous antenna gains, could have a systematic influence on range dependence of the reflectivity. Since very few elevation angles would be above that of the peak antenna gain at 8 MHz, and since the
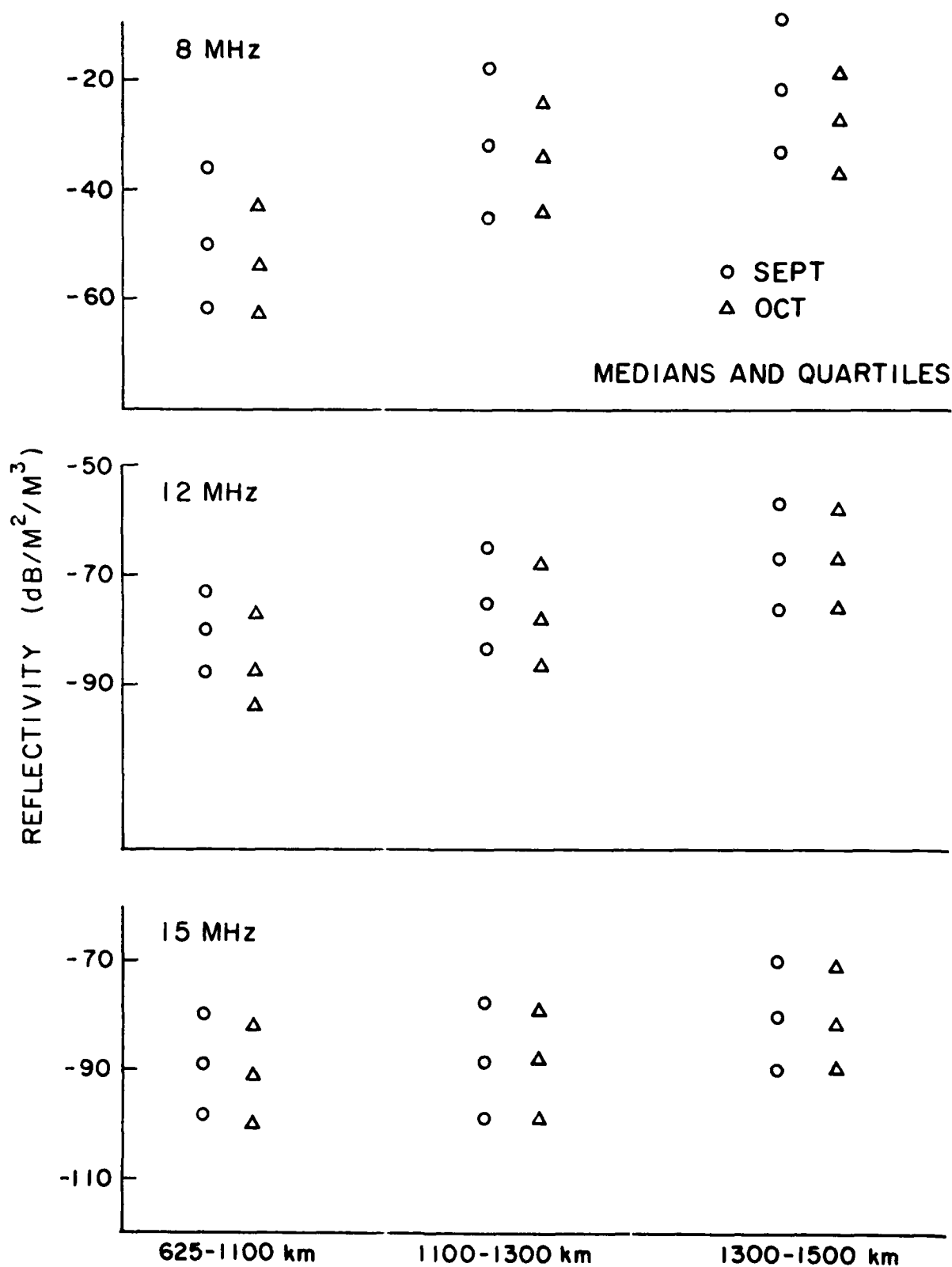
23

Figure 11. F Region Reflectivities vs. Range

24

dominant error was to underestimate the reflection height and thus under-
estimate the elevation angle and antenna gain for shorter ranges, any
systematic error in the reflectivity would be on the high rather than the
low side.

Also it seems possible that returns from the closest ranges could be
scattered back from nonorthogonal reflections. A consistent off-
orthogonality of the closest F layer returns due to insufficient refrac-
tion could lead to a reduced amplitude at the shortest ranges. Estimates
of the decrease in amplitude for off-orthogonal reflections run to 6 dB/deg.
Table 2 shows reflectivities of F layer clutter listed against frequency
and range. The reflectivities are listed separately for each of the four
sets of conditions being considered. In each listing the change in
reflectivity with frequency, in $m^2/m^3/km$ is listed for each frequency.
This shows that change of reflectivity with range is larger at the lower
frequencies, contradicting the expected behavior for the above orthogonality
related variation.

5.2 Frequency Dependence of Reflectivity

While a spatial variation in reflectivity is usually interpreted
as corresponding to the spatial distribution of the irregularities producing
the clutter, a frequency dependence should correspond to an intrinsic
property of the clutter source. The frequency dependence relates theoreti-
cally to the relative intensity of irregularities of different sizes. A
given wavelength of incident radiation is reflected according to the presence
of corresponding size irregularities. Much theoretical work has been done
to relate the structure of the irregularities, shown in the frequency
dependence of the scattered radiation, to the plasma instability models
proposed to explain the irregularities [R. A. Greenwald, 1975; M. D'Angelo,
1975]. However the models have been developed initially to explain
irregularities generated in the E region by the equatorial electrojet; and
attempts have been made to extend them to the auroral electrojet. There
has been much less progress in developing models of F region irregularities,
especially at high latitudes. Some current two-stream and gradient drift
models predict a power spectrum for the scattered radiation of the form

TABLE 2

F-Region Volume Reflectivities

(Azimuthal Averages)

Condition	Freq.	Evening Reflectivity (-dB/M^2/M^3)				Midnight Reflectivity (-dB/M^2/M^3)			
		Range Interval (Km)			Range Var. (dB/Km)	Range Interval (Km)			Range Var. (dB/Km)
		625-1100	1100-1300	1300-1500		625-1100	1100-1300	1300-1500	
Active	8	47	31	27	.038	52	34	27	.047
	12	79	68	60	.035	85	77	65	.036
	15	84	77	75	.017	90	87	79	.019
Wavenumber Exponent		14.1	17.3	14.5		14.5	20	19.3	
Quiet	8	62	48	37	.045	55	32	24	.059
	12	87	80	70	.030	92	83	69	.041
	15	90	83	82	.015	99	99	83	.026
Wavenumber Exponent		10.7	13.4	16.7		16.7	25	22	

26

$P \sim k^{-n}$, where k is the magnitude of the wave vector, with n = 3.-3.5
[Chestnut, 1968; Leadabrand, Larson and Hodges, 1967]. However, some
measurements show a wider range of values for this power law exponent
depending on conditions and the frequency of the scattered radiation.

5.2.1 E Reflectivities

For the purpose of studying the frequency dependence of reflectivity,
both the E layer and F layer reflectivities were averaged over azimuth.
The frequency dependence of the E layer reflectivities is shown in Figure 12
for each of the four conditions established above. While the active
midnight reflectivities are somewhat higher than those under other condi-
tions, the trend in all cases is very similar. The power law exponent for
these reflectivities has the exceptionally high value of 16, as opposed to
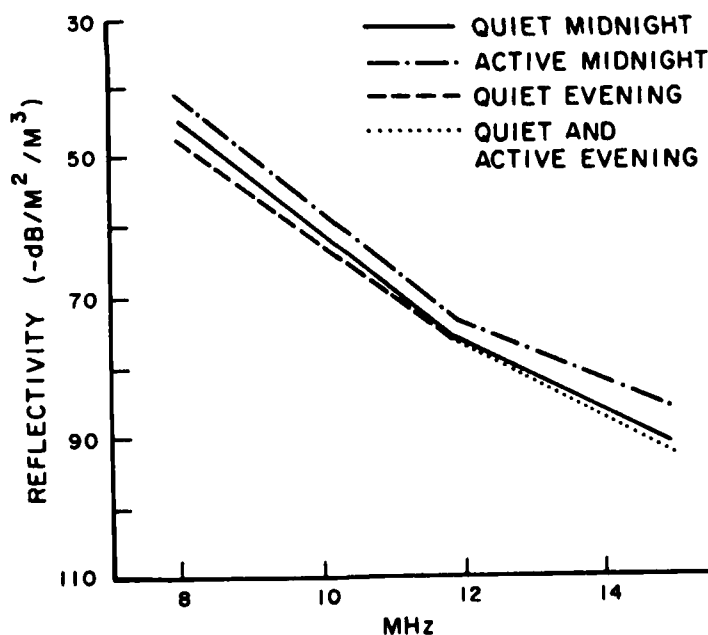the theoretical value on the order of 3.

Figure 12. E Layer Reflectivity vs. Frequency

The E layer reflectivities shown in Figure 13 for September and October are averaged over the four sets of conditions as well as over azimuth. Here the 19 MHz data for October was included to compare with corresponding data from September. There was no 10 MHz data in October. The frequency dependence of the E layer reflectivity is very similar for the two months with no consistent differences.

F Reflectivities

Table 1 shows, in addition to the range variation in reflectivity referred to above, the variation in reflectivity with frequency. These quantities, estimates of the exponent in the power law, are listed under each column of reflectivities at constant range. Again, no systematic variation with range or geomagnetic location is apparent. These values are on the order of those computed for the E layer clutter. F reflectivities averaged over range and the different sets of conditions are plotted against frequency in Figure 14 for the months of September and October. The value of the exponent for September is again about 16, with the October value being slightly smaller. This figure also shows a difference of 6 dB or less between the median E and F reflectivities at any of the 5 frequencies.

6. SUMMARY

Estimates have been computed, from a large sample of data, of HF volume backscatter reflectivities as a function layer height, geomagnetic coordinates, auroral conditions and frequency. F layer reflectivities were computed as a function of azimuth, range and local time. While there was a strong range dependence at all azimuth positions the range, azimuth and time variations could not be clearly coordinated with a set of geomagnetic coordinates. The source of the similar range variation at all azimuths, with no apparent geomagnetic correlation is not clear. A number of possible causes related to the radar system and analysis procedures were investigated and were found to be unlikely. E layer reflectivities were computed in only one range interval. These showed a somewhat more positive correlation with geomagnetic coordinates and auroral conditions, tending to be larger at those positions
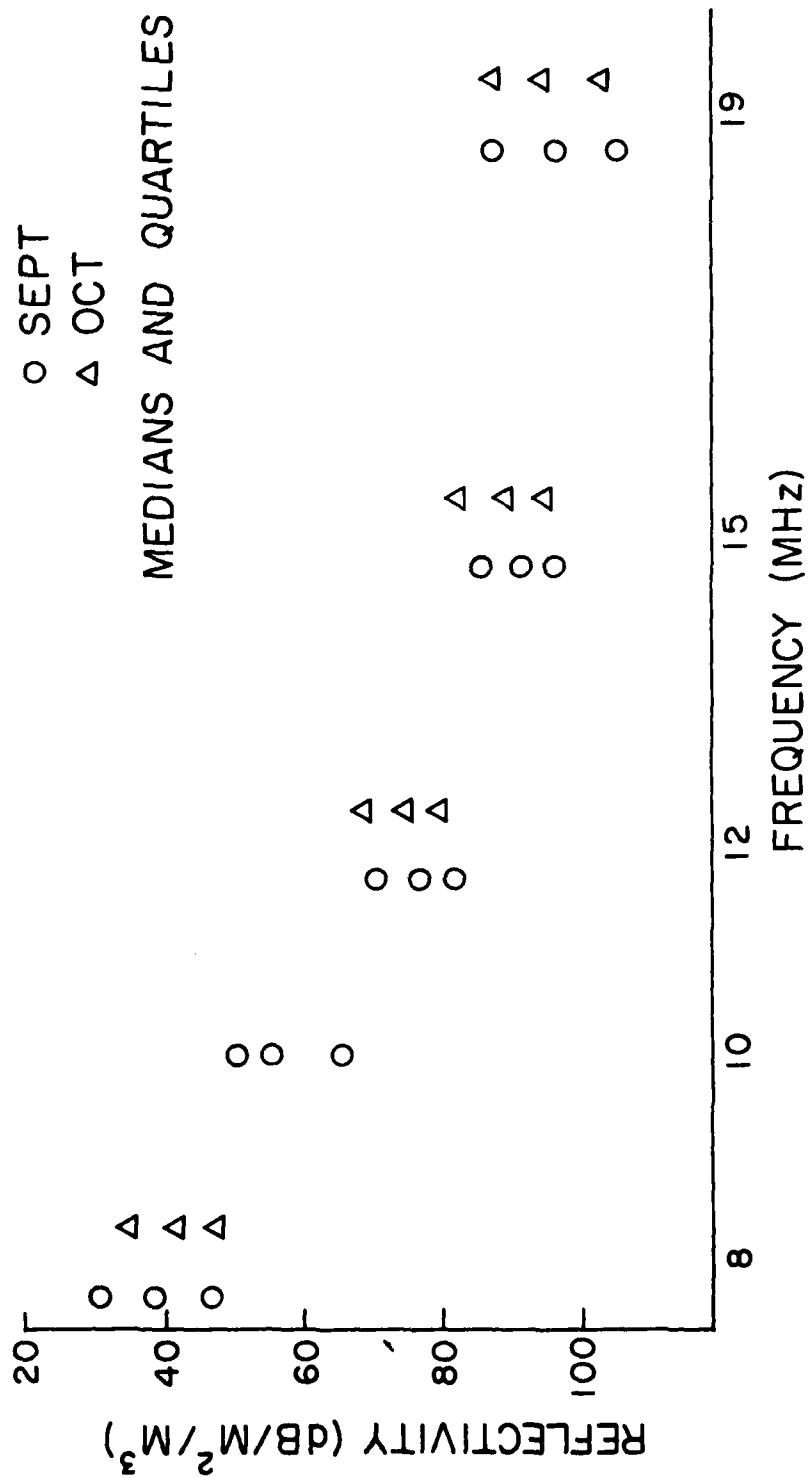
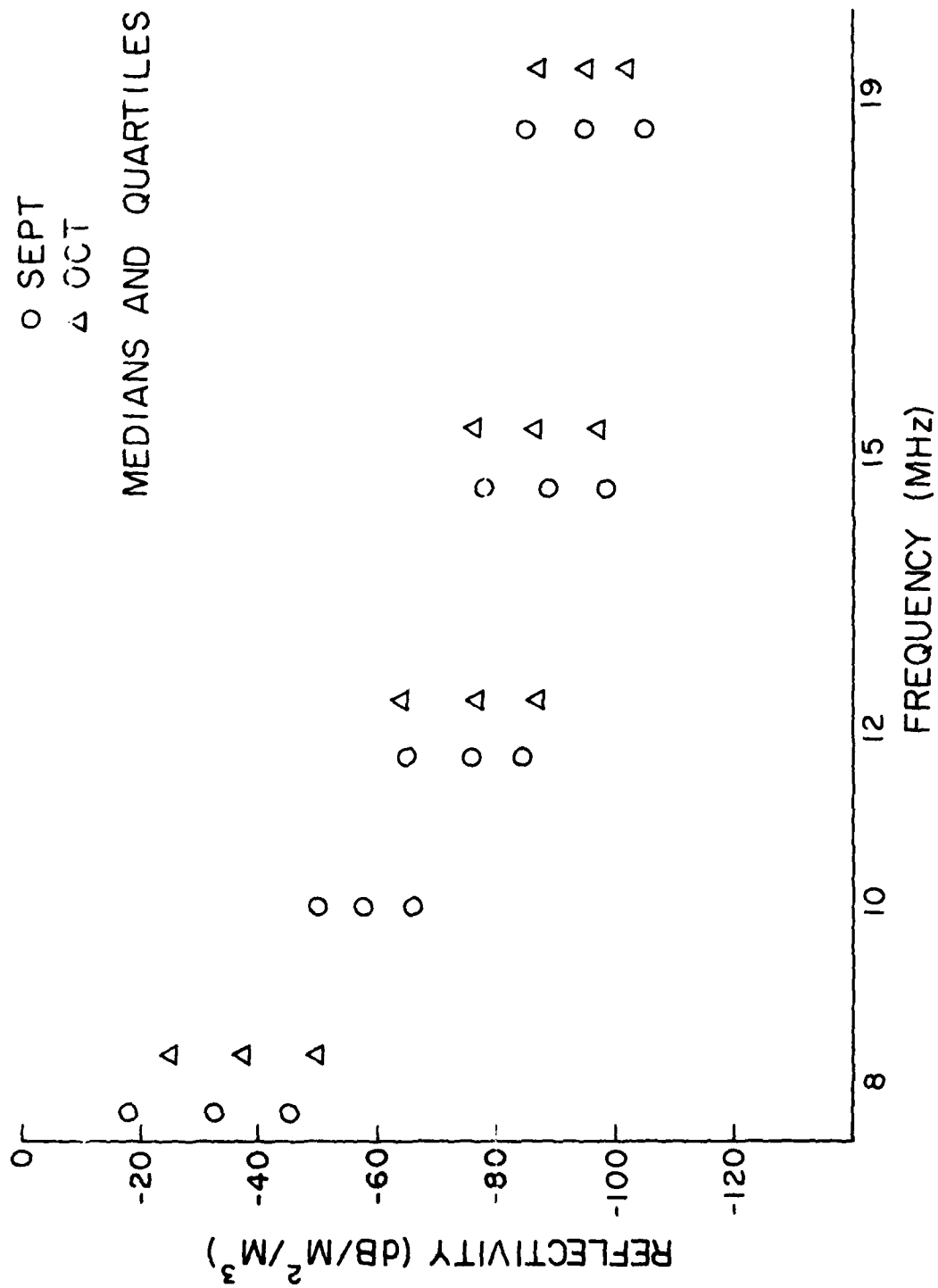Figure 15. E Layer Reflectivities vs. Frequency for September and October

Figure 14. F Layer Reflectivities vs. Frequency for September and October

covered by the auroral oval. The magnitudes of the E and F layer reflectivities, connected for both D region and auroral absorption, were very close for the same range interval.

Azimuthal averages of E and F layer reflectivities were compared for the months of September and October. The frequency variation of both the E and F layer reflectivities showed a close correspondence for the two months, as did the range variation in the F layer reflectivities.

The analysis presented here is probably weakened by the lack of detailed ionospheric information. This necessitated the assumption of straight line propagation in computing ray paths and reflection heights and volumes. While this renders the values of the reflectivities uncertain, no unexpected systematic behavior in the reflectivities could be traced to this source.

REFERENCES

Aarons, J., "A Descriptive Model of F Layer High-Latitude Irregularities as Shown by Scintillation Observations", J. Geophys. Res. (1973), 78, 7441.

Bullough, K. and T. R. Kaiser, "Radio Reflections from Auroral-II", J. Atm. Terr. Phys. (1955), 6, 198.

Chestnut, W. G., J. C. Hodges and R. L. Leadabrand, "Auroral Backscatter Wavelength Dependence Studies", Stanford Research Institute, Final Report, Contract AF30(602)-3734, June, 1968.

Farley, D. T., "A Plasma Instability Resulting in Field-Aligned Irregularities in the Ionosphere", J. Geophys. Res. (1963), 68, 6083.

Farley, D. T. and B. B. Balsley, "Instabilities in the Equatorial Electrojet", J. Geophys. Res. (1973), 78, 227.

Foppiano, A., "A New Method for Predicting the Auroral Absorption of H. F. Sky Waves", CCIR, IWP (1975) 6/1, Docs. 3 and 10.

George, P. L. and P. A. Bradley, "A New Method of Predicting the Ionospheric Absorption of High Frequency Waves at Oblique Incidence", ITU Telecommunications Journal, Geneva, May, 1974.

Ginzburg, V. L., The Propagation of Electromagnetic Waves in Plasmas, Pergamon Press, Oxford, 1970.

Ginzburg, V. L. and A. A. Ruhadze, "Waves and Resonances in Magneto-active Plasmas" in S. Fliigge, Encyclopedia of Physics 49/4, Springer-Verlag, New York, 1972.

Leadabrand, R. L., A. G. Larson and J. C. Hodges, "Preliminary Results on the Wavelength Dependence and Aspect Sensitivity of Radar Auroral Echoes between 50 and 3000 MHz", J. Geophys. Res. (1967), 72, 3877.

Martin, E. and J. Aarons, "F Layer Scintillations and the Aurora", J. Geophys. Res. (1977), 82, 2717.

REFERENCES (Cont.)

Nichols, B. E., "Propagation Measurements Program (Polar Fox II) Antenna
Patterns and Gains", Lincoln Laboratory Project Report PMP 6, ESD
Contract F19628-73-C-0002, July, 1973.

Nielson, E. and J. Aarons, "Satellite Scintillation Observations over the
Northern High Latitude Regions", J. Atm. Terr. Phys. (1974) 36, 159.

Parry, J. L., "Antenna Pattern Measurements", Project 1765, Rome Air
Development Center, RADC-TR-73-32, March, 1973. AD 909 689L.

Preanell, R. I., R. L. Leadabrand, A. M. Peterson, R. B. Dyce, J. C.
Schlobohm and M. R. Berg, "VHF and UHF Radar Observations of the
Aurora at College, Alaska", J. Geophys. Res. (1959) 64, 1179.

Rogister, A. and M. D'Angelo, "Type II Irregularities in the Equatorial
Electrojet", J. Geophys. Res. (1973) 75, 6808.

Unger, J. H. W., R. H. Hardin and R. J. Horan, "Auroral Clutter in UHF
Radar", Bell Laboratories Advanced Ballistic Missile Defense Agency,
Contract DAHC 60-69-0008, Oct., 1973.

Unwin, R. S. and W. J. Baggeley, "The Radio Aurora", Annales de Geophysique
(1972) 28, 111.

Vondrak, R. R., G. Smith, V. E. Hatfield, R. T. Tsunada, V. R. Frank and
P. D. Perreault, "Chatanika Model of the High Latitude Ionosphere
for Application to H. F. Propagation Prediction", S.R.I. Inter-
national, RADC-TR-78-7 AD A053154, Jan., 1978.

MISSION
of
Rome Air Development Center

RADC plans and executes research, development, test and selected acquisition programs in support of Command, Control Communications and Intelligence (C^3I) activities. Technical and engineering support within areas of technical competence is provided to ESD Program Offices (POs) and other ESD elements. The principal technical mission areas are communications, electromagnetic guidance and control, surveillance of ground and aerospace objects, intelligence data collection and handling, information system technology, ionospheric propagation, solid state sciences, microwave physics and electronic reliability, maintainability and compatibility.